Transmission and frequency spectra of acoustic phonons in Thue-Morse superlattices

S. Tamura
Department of Engineering Science, Hokkaido University, Sapporo, Hokkaido 060, Japan

Franco Nori*
Institute for Theoretical Physics, University of California, Santa Barbara, Santa Barbara, California 93106
(Received 8 May 1989)

We study the transmission and frequency spectra of phonons in aperiodic Thue-Morse superlattices. Calculations based on the transfer-matrix method predict rich structures of the transmission dips and frequency gaps, and their basic properties are well described by the superlattice-structure factors that we derive. The angular dependence of the phonon transmission is also calculated and the existence of the intermode reflection of phonons is confirmed. Our results indicate that in the single-layer superlattice the spectral structures of phonons associated with the nonperiodicity of the Thue-Morse sequence dominate those arising from the underlying periodicity. This suggests that, for an experimental verification of the phonon spectra unique to the aperiodic nature of the sequence, the single-layer superlattice is more appropriate than the double-layer one. The latter exhibits a significant correlation with a corresponding periodic superlattice in the spectral dips and gaps.

I. INTRODUCTION

The pioneering work of Merlin *et al.*[1] on Fibonacci GaAs/AlAs superlattices (SL's) has generated a large amount of research activity on both electronic and vibrational properties of systems with quasiperiodic order.[2] More recently, the studies on acoustic-phonon transmission[3] and especially on the angular dependence of phonon transmission[4] through a Fibonacci SL have produced theoretical and experimental results which are quite similar to the ones previously obtained for the phonon transmission spectra in conventional periodic SL's.[5] Several reasons contribute to this situation. One of them is related to the limited resolution of the currently available phonon detectors. Fine structure in the spectra, present in the Fibonacci case but absent in the periodic case, is difficult to resolve experimentally. Furthermore, even at the theoretical level the results do agree remarkably well (again, specially for the main overall features). The kind of ordering present in a Fibonacci SL is called "quasiperiodic" which, as the name suggests, is a slight variation of the periodic ordering. In order to explore the effects of the lack of translational invariance on phonon propagation in SL's, we need to consider more than just weak aperiodicity.

The study of the acoustic-phonon transmission through a realistic Thue-Morse SL is motivated by the fact that this deterministic structure is more "disordered" than the quasiperiodic one.[6,7] In other words, this system has a degree of aperiodicity intermediate between quasiperiodic and random. More precisely, the Fourier-amplitude spectrum of the Thue-Morse sequence does not have δ-function peaks. In contrast, the Fourier-amplitude spectrum of any quasiperiodic structure is composed only of δ-function peaks. Of course, this is also the case for any periodic systems. Using a more accurate terminology, neither singular nor absolutely continuous components are present in the Fourier spectra of the quasiperiodic and periodic chains, while the spectrum of the Thue-Morse sequence has only a singular continuous component.[8]

The first experimental realization of a Thue-Morse GaAs/AlAs SL which stimulates the present work is due to Merlin *et al.*[9] Other recent works related to the Thue-Morse sequence include a quantum-mechanical Ising model in a transverse magnetic field,[10] a linear-chain model for lattice vibration,[11] and tight-binding models for electrons.[12,13] One of the basic questions is how does the lack of translational invariance, in general, and the Thue-Morse ordering (with its Fourier spectra without δ peaks), in particular, affect the phonon transmission in a realistic SL? The effect of aperiodicity has not been fully explored so far since previous works in this area were restricted to weakly aperiodic (quasiperiodic) structures.[3,4] In order to answer this issue, we shall study both the transmission rate and dispersion relation of phonons propagating normal to the interfaces of Thue-Morse SL's. They should provide complementary information on the spectral properties of phonons characteristic of these aperiodic systems, which is accessible by phonon spectroscopy experiments. More detailed information on the spectral properties of phonons will be obtained through the angular dependence of the transmission for phonons propagating oblique to the SL interfaces. All these calculations for the Thue-Morse SL will indeed reveal a number of spectral structures quite different from those in the periodic SL's, yet identifiable based on the SL-structure factors we shall derive analytically.

In the next section we summarize information on the Thue-Morse sequence in order to make this paper self-

 ©1989 The American Physical Society

contained. The structure factors of the Thue-Morse SL's appropriate to the phonon problem are derived in Sec. III for both double- and single-layer systems. The corresponding expressions for the structure factors in the periodic SL's are also presented. The transmission and frequency spectra of phonons in AlAs/GaAs SL's based on the Thue-Morse sequence are given in Secs. IV and V, respectively, for the propagation normal to the interfaces of both the single- and double-layer SL's. The angular dependence of the phonon transmission is shown in Sec. VI. The characteristic structures of all these phonon spectra obtained numerically are explainable in terms of the structure factors of the Thue-Morse SL's given in Sec. III. We summarize our results in Sec. VII.

II. THE THUE-MORSE CHAIN

The Thue-Morse sequence of order (or generation) N has 2^N elements over the alphabet $\{0,1\}$, defined recursively as follows:[6,7]

$$\epsilon_{2n}=\epsilon_n \text{ and } \epsilon_{2n+1}=1-\epsilon_n \ , \tag{1}$$

for integer $n \geq 0$ with $\epsilon_0=0$. The above recursion equations generate, as $n \rightarrow \infty$, an infinite string of (binary) digits (0 or 1) which never repeats itself. In spite of this aperiodicity, the Thue-Morse sequence is self-similar. Furthermore, and unlike the quasiperiodic case, the Thue-Morse chain cannot be characterized by a finite set of irrational numbers.

The sequence of some Thue-Morse SL parameters, for instance, the thickness of each type of layer (d_A and d_B) is obtained by associating with every 1 and 0 of the above sequence the values $d_A=d$ $d_B=cd$ respectively. Therefore, the deviation of c from unity conveniently gauges the lack of translational invariance in the system. In other words, our results will obviously depend on the choice of c. Clearly, the $c \rightarrow 1$ limit corresponds to the usual periodic regime, while the limits $c \ll 1$ and $c \gg 1$ correspond to the strongly aperiodic regimes. Of course, numerical computations cannot handle the infinite aperiodic chain, however, the aperiodic Thue-Morse structure can be conveniently approximated by a sequence of chains with progressively larger unit cells of size 2^N and periodic boundary conditions.

Successive generations of the Fibonacci and Thue-Morse sequences are both obtained by iteration of the extremely simple (concurrent) substitutions: (i) $0 \rightarrow 01$ and $1 \rightarrow 0$ (under the Fibonacci construction) and (ii) $0 \rightarrow 01$ and $1 \rightarrow 10$ (under the Thue-Morse construction). The former has been recently studied and discussed by many authors in the recent physics literature.[2] However, the latter is relatively unknown to most physicists; therefore some background information on it might be appropriate.

Sequences generated by reiteration of (concurrent) substitutions have been studied in several areas of mathematics, computer science, cryptography, and, more recently, physics. One of the first systematic studies of aperiodic sequences was made by Thue[6] in 1906. His results have been rediscovered many times since then. In most cases, those "new" rediscoveries have been made in completely different disciplines. Morse[7] studied substitution-generated sequences in the context of topological dynamics. Others have analyzed them in such diverse topics as (i) ergodic theory,[14] (ii) automata theory (tag machines, characterization of recognizable sets of numbers),[15] (iii) formal language theory,[16] (iv) solutions to algebraic equations,[17] and (v) combinatorial theory.[18] This multiplicity of rediscoveries has yielded many different ways to define the Thue-Morse sequence. We will only mention here the simplest ways to generate it. The recurrence relation definition has been presented in Eq. (1). Alternatively, let γ_n be the number of 1's in the binary representation of the integer n. Thus,

$$\epsilon_n=[1-(-1)^{\gamma_n}]/2 \ . \tag{2}$$

Yet another definition starts with the sequence of positive integers. After writing them in the binary representation, we sum the digits of every integer modulo 2 and obtain the Thue-Morse (TM) sequence. On the other hand, the so-called "word concatenation" approach starts with $W_0=0$, and defines $W_{N+1}=W_N\overline{W}_N$, for $N \geq 0$ where $\overline{W}_N$ is obtained from W_N by replacing every 0 with 1 and vice versa. Thus, $W_1=01$, $W_2=0110$, $W_3=01101001$, $W_4=0110100110010110$, and so on. By omitting every other digit in a given sequence,—i.e., "decimation"—we obtain 01101001 ($=W_3$), which is none other than the string of the preceding generation. In other words, the infinite TM sequence is not only aperiodic, but also self-similar. Thus, the usual symmetry, translational invariance, has been replaced by the invariance with respect to multiplicative changes of scale (i.e., scaling invariance). The scaling factor is, of course, equal to 2. Periodicity has always provided a useful tool to understand and simplify the formulation of physical problems (e.g., Bloch's theorem, crystal-momentum conservation). Of course, for aperiodic sequences, these tools become inapplicable. However, the concept of "periodicity" is still lurking behind (in a subtle way) the Thue-Morse construction because "scale invariance" is nothing other than "periodicity on a logarithmic scale."

III. STRUCTURE FACTORS OF THUE-MORSE SUPERLATTICES

Similar to the cases of periodic and quasiperiodic SL's, the properties of the transmission and frequency spectra of phonons in Thue-Morse SL's are gained by studying the SL-structure factors which properly describe the interference effects of the phonons reflected at the interfaces of constituent layers.[19–21] Here we shall consider the structure factors for the following two kinds of Thue-Morse SL's appropriate for phonon problems.

A. Double-layer superlattice

The double-layer SL consists of two building blocks (A and B), each one of them composed, in general, of two kinds of layers with different elastic properties and different thicknesses. This is the simplest case of multilayer SL's in which the interfaces between consecutive AA (BB) blocks in the sequence are well defined. A

schematic double-layer Thue-Morse SL is shown in Fig. 1(a). We assume that the first (second) layers of both A and B blocks are composed of the same materials. For instance, AlAs and GaAs will be chosen as the first and second layers of each block. Furthermore, it is assumed that the substrate of the SL and the thin-film phonon detector deposited on the other surface of the SL has the same elastic properties as the second layer of building blocks. This means that phonons are totally transmitted from the top layer of the SL into the detector, although their transmisison is only partial between the substrate and the SL.

Provided that the interfaces of a SL are the mirror-symmetry planes of the constituent crystalline materials, all three modes of phonons propagating normal to the SL are decoupled from each other. Thus for the normal incidence of phonons only intramode reflection and transmission occur at interfaces and the amplitude-reflection coefficient r_{21} for a phonon impinging on an interface from the second-layer takes the form[20]

$$r_{21}=\frac{Z_2-Z_1}{Z_2+Z_1}\ , \tag{3}$$

where the acoustic impedances Z_n $(n=1,2)$ are defined by $Z_n=\rho_n v_n$ with ρ_n the mass density and v_n the sound velocity. Next, we define $a_n=2k_n d_n^A=2\omega d_n^A/v_n$ and $b_n=2k_n d_n^B=2\omega d_n^B/v_n$, where k_n are the wave numbers, ω is the angular frequency, and d_n^A and d_n^B are the thicknesses of the layers of A and B blocks, respectively. Taking the SL structure shown in Fig. 1(a) into account, we find the following recursion relations satisfied by the structure factor $S_N^{\rm TM}$ of the double-layer Thue-Morse SL

$$S_{N+1}^{\rm TM}(\omega)=S_N^{\rm TM}(\omega)+\bar{S}_N^{\rm TM}(\omega)\exp[2^{N-1}i(a+b)]\ , \tag{4a}$$

$$\bar{S}_{N+1}^{\rm TM}(\omega)=\bar{S}_N^{\rm TM}(\omega)+S_N^{\rm TM}(\omega)\exp[2^{N-1}i(a+b)]\ ,\quad \text{for } N\geq 1\ ; \tag{4b}$$

$$S_1^{\rm TM}(\omega)=r_{21}[h_A(\omega)+h_B(\omega)e^{ia}]\ , \tag{4c}$$

where N is the generation number, $h_A=1-\exp(ia_1)$, $h_B=1-\exp(ib_1)$, $a=a_1+a_2$, $b=b_1+b_2$, and $\bar{S}_N^{\rm TM}$ is the "complement" of $S_N^{\rm TM}$ obtained by interchanging in $S_N^{\rm TM}$ the variables characterizing A and B blocks. In the following we assume that the first layers of both A and B blocks have the same thickness, i.e., $d_1^A=d_1^B$, but $d_2^A\neq d_2^B$. This means that $a_1=b_1$ and we define $h=h_A=h_B$.

Now, solving Eq. (4), we have

$$|S_N^{\rm TM}(\omega)|^2=4^{N-2}r_{21}^2\left|f_+(\omega)\prod_{n=1}^{N-1}\cos[2^{n-2}(a+b)]+(-i)^{N-1}f_-(\omega)\prod_{n=1}^{N-1}\sin[2^{n-2}(a+b)]\right|^2,\quad N\geq 2\ , \tag{5a}$$

with

$$|S_1^{\rm TM}(\omega)|^2=r_{21}^2|f(\omega)|^2\ , \tag{5b}$$

where the factors $f_\pm$ and $f=(f_++f_-)/2$ represent modulation effects on acoustic fields due to the internal structures of the building blocks and explicitly they are given by

$$f_+(\omega)=h(\omega)(2+e^{ia}+e^{ib})\ ,\qquad f_-(\omega)=h(\omega)(e^{ia}-e^{ib})\ . \tag{6}$$

For comparison's sake, here we give a similar expression for the structure factor S_N^P of an associated periodic, double-layer SL consisting of the sequence $ABABAB\cdots$,

$$|S_N^P(\omega)|^2=4^{N-1}r_{21}^2\left|f(\omega)\prod_{n=1}^{N-1}\cos[2^{n-2}(a+b)]\right|^2,\quad N\geq 2\ , \tag{7a}$$

with

$$|S_1^P|^2=|S_1^{\rm TM}|^2\ . \tag{7b}$$

Comparing Eq. (5) with the structure factor given by Cheng *et al.* [Eq. (9) of Ref. 13], we recognize that the basic properties of the structure factor for the linear Thue-Morse chain are also valid for the structure factor of the double-layer Thue-Morse SL. The most obvious feature deduced from Eq. (5) is the Bragg reflection of phonons in the Thue-Morse SL, which occurs at the same frequencies as in the periodic system. (Its existence is, however, not recognized in the expression of the structure factor derived by Cheng *et al.*[13]) This basically arises from the fact that the Thue-Morse SL is constructed by arranging two kinds of double blocks AB and BA so that the resulting array of the blocks may form a Thue-Morse sequence. The same amount of the phase of $(a+b)/2$ is added to acoustic fields after the perfect transmission of phonons through these double blocks. This implies that the phonons with frequencies satisfying

$$a+b=2m\pi,\quad m=1,2,3,\ldots \tag{8}$$

are strongly reflected in this nonperiodic SL. Equation (8) is the same condition as the Bragg condition for phonons in the periodic SL defined above. Thus we can regard that the Thue-Morse SL effectively has a periodicity not explicitly seen in its sequence.

Now in the double-layer SL the Bragg condition (8) is satisfied at frequency $\omega=\omega_m$, where

$$\omega_m=\frac{m\pi}{(d_1^A+d_1^B)/v_1+(d_2^A+d_2^B)/v_2} \tag{9}$$

and the index m indicates the order of the reflection. At these frequencies Eqs. (5) and (7) are reduced to

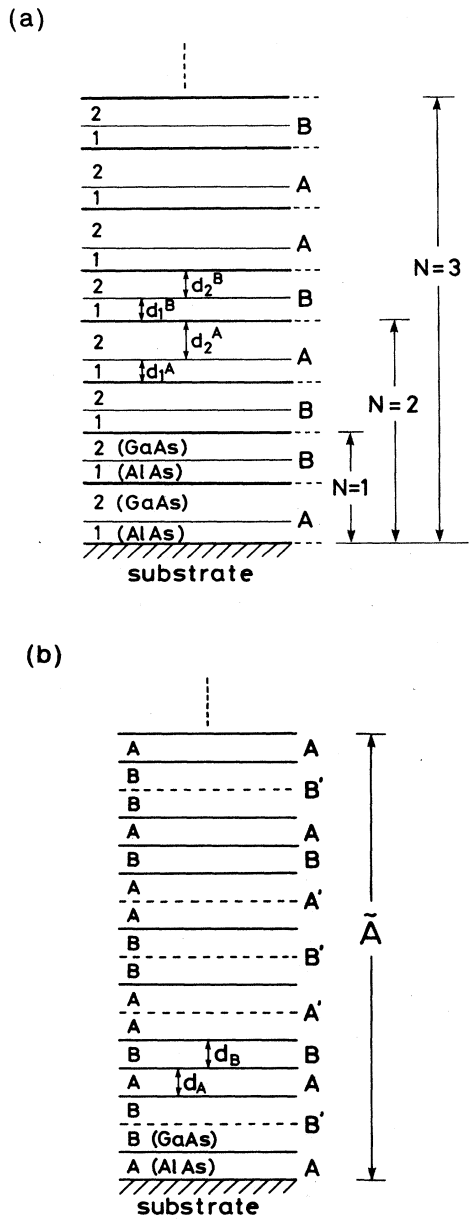

FIG. 1. Schematic Thue-Morse superlattice (SL) systems consisting of building blocks A and B. (a) Double-layer SL in which each building block has two layers of different materials. (The first three generations are shown.) The constituent materials of the first (also the second) layers in both A and B blocks are assumed to be the same but with different thicknesses (denoted by d_1^A and d_1^B for the first layers and d_2^A and d_2^B for the second layers) in general. AlAs and GaAs are assumed for the constituents of the first and second layers in the numerical examples. (b) Single-layer SL in which both A and B blocks are composed of one layer of different materials with thicknesses d_A and d_B. In this SL, adjoining AA and BB blocks should be treated as new building blocks and are denoted by A' and B', respectively. A large $\tilde{A}$ consisting of 16 original A and B blocks is regarded as an effective unit block of the sequence (see the text). AlAs and GaAs are assumed for the constituents of A and B blocks in the numerical calculation.

$$|S_N^{\mathrm{TM}}(\omega_m)|^2=4^{N-1}r_{21}^2|f_+(\omega_m)/2|^2 ,$$
$$|S_N^P(\omega_m)|^2=4^{N-1}r_{21}^2|f(\omega_m)|^2 . \tag{10}$$

Hence, the spectral intensities at Bragg frequencies ω_m grow as 4^N with increasing the generation number N. At these frequencies the magnitude of the spectral peaks in the Thue-Morse SL relative to the periodic SL becomes

$$\left|\frac{f_+(\omega_m)}{2f(\omega_m)}\right|^2=\frac{1+\cos a_m}{2} , \tag{11}$$

where $a_m=a(\omega=\omega_m)$. Equation (11) means that $|S_N^P(\omega_m)|^2\geq|S_N^{\mathrm{TM}}(\omega_m)|^2$ for double-layer SL's. Thus we can expect that at ω_m, the magnitude of transmission dips as well as the width of frequency gaps in the periodic SL are larger than or equal to those in the Thue-Morse SL. This will be confirmed numerically in Sec. VI.

The spectral properties truly characteristic of the Thue-Morse SL appear at $\omega_{m/3}\equiv\omega_m/3$ $(m\neq 3n)$. The existence of peaks of the structure factor at these frequencies was found by Cheng *et al.*[13] by studying the scaling properties of the spectral intensity in the linear Thue-Morse chain. At $\omega_{m/3}$,

$$|\cos[2^n(a+b)]|=\tfrac{1}{2}<|\sin[2^n(a+b)]|=\sqrt{3}/2$$

holds, and hence for a large generation number N we find

$$|S_N^{\mathrm{TM}}(\omega_{m/3})|^2=3^{N-1}r_{21}^2|f_-(\omega_{m/3})/2|^2 . \tag{12}$$

Accordingly, the spectral intensities at $\omega_{m/3}$ increase in proportion to 3^N with increasing the generation number N, which is much slower than the 4^N behavior at ω_m. Next we define the scaling exponent $\eta(\omega)$ in the limit of large N by

$$|S_N^{\mathrm{TM}}(\omega)|^2=L^{\eta(\omega)} , \tag{13}$$

where $L=2^N$ is the effective size of the system. Then it is deduced that $\eta(\omega_m)=2$ and $\eta(\omega_{m/3})=\ln 3/\ln 2=1.585\cdots$, and the latter exponent has been proven to be the largest nontrivial exponent other than the former associated with the Bragg reflection.[13]

Several basic properties of the scaling exponents for the Thue-Morse chain which are equally applicable to the SL systems have been derived.[13] One of the relevant properties to our problem is that $\eta(\omega_x)=\eta(\omega_y)$ if $\Delta=x-y$ (mod1) has a finite-length binary representation, where ω_x and ω_y are defined by Eq. (9) with m replaced by x and y, respectively. For instance, $\Delta=\pm\frac{1}{2}$ have the shortest length and $\Delta=\pm\frac{1}{4}$ (also $\pm\frac{3}{4}$) have the second shortest length binary representations, and so on. Accordingly, besides the spectral peaks at ω_m only those peaks at $\omega_{m/3}$ as well as those related to the frequencies $\omega_{m/3+\Delta}$ should persist for the Thue-Morse SL with a large generation. All these predictions will be confirmed by the numerical results for the transmission and frequency spectra of phonons developed in the next section.

B. Single-layer superlattice

The Thue-Morse SL realized by Merlin *et al.*[9] consists of the sequence of two-single-layer building blocks A and

B with thicknesses d_A and d_B, respectively. Because phonons cannot recognize the existence of the interfaces between consecutive AA and BB blocks in this system, we should regard these double blocks as new units and denote the former and latter blocks by A' and B', respectively. A close examination reveals that the sequence of eleven blocks $AB'ABA'B'A'BAB'A$ shown in Fig. 1(b) (which consists of sixteen original A and B blocks) is to be chosen as the unit of the single-layer Thue-Morse SL. We denote this large unit block by $\tilde{A}$ (the zeroth generation). Then we find that the first generation ($N=1$) consists of the block $\tilde{A}$ concatenated with its complement $\tilde{B}$. Similarly, the higher generations comprise arrangements of $\tilde{A}$ and $\tilde{B}$ blocks following the Thue-Morse sequence, i.e., $\tilde{A}\tilde{B}\tilde{B}\tilde{A}\tilde{B}\tilde{A}\tilde{A}\tilde{B}\cdots$.

Now, it is assumed that both the substrate and phonon detector attached to each other on the opposite sides of this SL system have the same elastic properties as the constituent of B block. Under this assumption we can also derive the recursion relations satisfied by the structure factor s_N^{TM} and its complement $\bar{s}_N^{\mathrm{TM}}$ of the single-layer SL

$$s_{N+1}^{\mathrm{TM}}(\omega)=s_N^{\mathrm{TM}}(\omega)+\bar{s}_N^{\mathrm{TM}}(\omega)\exp[2^{N+2}i(\alpha+\beta)]\ , \tag{14a}$$

$$\bar{s}_{N+1}^{\mathrm{TM}}(\omega)=\bar{s}_N^{\mathrm{TM}}(\omega)+s_N^{\mathrm{TM}}(\omega)\exp[2^{N+2}i(\alpha+\beta)]\ , \quad N\geq 0\ ; \tag{14b}$$

with

$$s_0^{\mathrm{TM}}(\omega)=r_{BA}[g_+(\omega)+g_-(\omega)]/2\ , \tag{14c}$$

where

$$\alpha=2k_Ad_A=2\omega d_A/v_A,\quad \beta=2k_Bd_B=2\omega d_B/v_B\ ,$$

r_{BA} is the amplitude-reflection coefficient at the interface between B and A blocks defined similarly as Eq. (3), and

$$\begin{aligned} g_+(\omega)&=(e^{i\beta}-e^{i\alpha})\sum_{n=0}^{7}e^{in(\alpha+\beta)}\ ,\\ g_-(\omega)&=(2-e^{i\alpha}-e^{i\beta})[1-e^{2i(\alpha+\beta)}+e^{6i(\alpha+\beta)}]\\ &\quad+(e^{i\alpha}+e^{i\beta})[e^{i(\alpha+\beta)}-e^{3i(\alpha+\beta)}\\ &\quad+e^{4i(\alpha+\beta)}-e^{5i(\alpha+\beta)}]\ . \end{aligned} \tag{15}$$

Solving Eq. (14), we have

$$|s_N^{\mathrm{TM}}(\omega)|^2=4^{N-1}r_{BA}^2\left|g_+(\omega)\prod_{n=1}^{N}\cos[2^{n+2}(\alpha+\beta)]+(-i)^Ng_-(\omega)\prod_{n=1}^{N}\sin[2^{n+2}(\alpha+\beta)]\right|^2,\quad N\geq 1\ . \tag{16}$$

This equation is similiar to Eq. (5) for the double-layer SL.

Here we shall give again the corresponding expression for the structure factor s_N^P of the periodic single-layer SL consisting of the sequence of alternating A and B blocks, i.e., $ABABAB\cdots$. For the coordination with the Thue-Morse SL we regard the periodic sequence involving 32 blocks (sixteen A blocks and sixteen B blocks) as the first generation, i.e., $N=1$, and we find

$$|s_N^P(\omega)|^2=4^Nr_{BA}^2\left|g(\omega)\prod_{n=1}^{N}\cos[2^{n+2}(\alpha+\beta)]\right|^2,\quad N\geq 1\ , \tag{17}$$

where $g=(g_++g_-)/2$ and explicitly

$$g(\omega)=(1-e^{i\alpha})\sum_{n=0}^{7}e^{in(\alpha+\beta)}\ . \tag{18}$$

In the single-layer Thue-Morse SL the Bragg reflection of phonons due to the implicit periodicity of the sequence occurs at the frequencies satisfying $\alpha+\beta=2m\pi$ or $\omega=\omega'_m$, where

$$\omega'_m=\frac{m\pi}{d_A/v_A+d_B/v_B},\quad m=1,2,3,\ldots\ . \tag{19}$$

At these frequencies Eqs. (16) and (17) become

$$|s_N^{\mathrm{TM}}(\omega'_m)|^2=4^Nr_{BA}^2|g_+(\omega'_m)/2|^2\ , \tag{20a}$$

$$|s_N^P(\omega'_m)|^2=4^Nr_{BA}^2|g(\omega'_m)|^2\ . \tag{20b}$$

Accordingly, the magnitude of the spectral intensities in the single-layer Thus-Morse SL relative to those in the periodic SL is given by

$$\left|\frac{g_+(\omega'_m)}{2g(\omega'_m)}\right|^2=\frac{1+\cos\alpha_m}{2}\ , \tag{21}$$

where $\alpha_m=\alpha(\omega'_m)$. Equation (21) predicts that also in the single-layer systems the spectral peaks at Bragg frequencies are always larger in the periodic SL than those in the Thue-Morse SL.

From Eq. (16) we find at $\omega'_{m/3}\equiv\omega'_{m/3}$ and for a large N

$$|s_N^{\mathrm{TM}}(\omega'_{m/3})|^2=3^N|r_{BA}^2g_-(\omega'_{m/3})/2|^2\ , \tag{22}$$

which should be compared to Eq. (12) for the double-layer SL. Thus we see that both the single- and double-layer SL's should exhibit the same fundamental spectral properties as those in the linear Thue-Morse chain.

IV. FREQUENCY DEPENDENCE OF TA-PHONON TRANSMISSION RATE

In order to verify the spectral properties of phonons in the Thue-Morse SL's predicted in Sec. III, we shall calculate the transmission rate of TA phonons propagating parallel to the growth direction. Here we note that with the use of phonon-spectroscopic methods the frequency dependence of the transmission was measured for both crystalline[22] and amorphous[23] SL's with regular periodicity. The significant dips in transmission which evidence

the Bragg reflection due to these artificially modulated periodicities were observed.

The calculation of transmission rates in the periodic and quasiperiodic SL's have been performed by using the transfer-matrix method.[3,5] The same kind of calculation will be applied to the Thue-Morse SL's, only the input sequence of building blocks needs to be changed. Figure 2(a) shows the result for a double-layer Thue-Morse SL, where we have assumed the (001)-oriented AlAs and GaAs as the first and second layers of both A and B blocks, respectively, and their thicknesses are $d_1^A = d_1^B = 17$ Å (AlAs layers), $d_2^A = 42$ Å, and $d_2^B = 20$ Å (GaAs layers). The fifth generation is assumed for the calculation. For higher generations the transmission dips present in this figure become more significant and additional small dips with narrower frequency widths appear densely. The apparently complicated distribution and magnitude of these transmission dips are, however, well understood in terms of the structure factor S_N^{TM} given by Eq. (5). The dips labeled by integers ($m = 1-8$) are attributed to Bragg reflections due to the underlying periodicity. This can be confirmed by comparing Fig. 2(a) with Fig. 2(b) which exhibits the transmission rate in the corresponding periodic system consisting of alternating A and B blocks. Those Bragg dips in the Thue-Morse and periodic SL's occur at the same frequencies ω_m at which the spectral intensities have peaks, and a remarkable correlation in their magnitude is clearly observed.

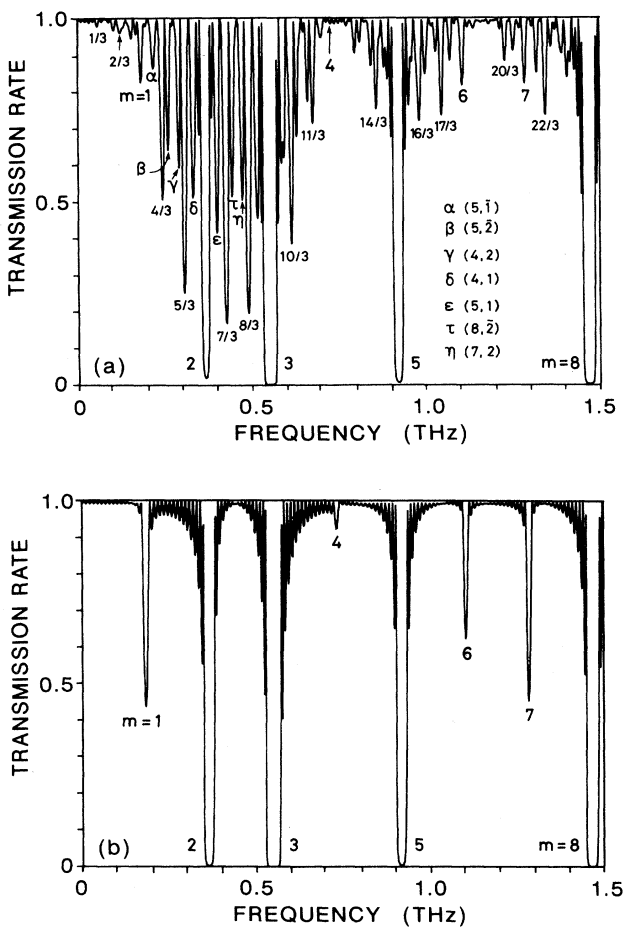

FIG. 2. Frequency dependence of TA-phonon transmission rate in double-layer (001)-oriented AlAs/GaAs SL's. Propagation is normal to the SL interfaces. (a) Thue-Morse SL. (b) Periodic SL. Layer thicknesses are $d_1^A = d_1^B = 17$ Å (AlAs layers), $d_2^A = 42$ Å, and $d_2^B = 20$ Å (GaAs layers) and the fifth generation with 32 blocks (64 layers) is assumed. Dips are labeled by the indices of the frequencies predicted by the structure factors (see the text).

The dips other than those resulting from Bragg reflection are ascribed to the nonperiodicity of the sequence and unique to the Thue-Morse SL. Several major dips are found at the frequencies $\omega_{m/3}$ ($m \neq 3n$) predicted by the property of the structure factor, and in Fig. 2(a) they are labeled by the associated fractional numbers $m/3$. The remaining dips can also be identified based on the discussion developed in Sec. III and are labeled by the sets of integers (m,k) or $(m,\bar{k})$, which define the frequencies ω_z at which they occur, where $z = m/3 + (\frac{1}{2})^k$ for the former set and $z = m/3 - (\frac{1}{2})^k$ for the latter set.

We are left to account for the relative magnitudes of the calculated transmission dips. They are related to the spectral intensity of the Thue-Morse SL and hence basically described by Eq. (5) as well. In Table I we have tabulated the magnitude of the spectral intensities of the Thue-Morse and periodic SL's at Bragg frequencies. These results are well in accord with the relative magnitudes of transmission dips not only within each SL but also between the Thue-Morse and periodic SL's. We have also given in Table II the spectral intensities at $\omega_{m/3}$ ($m \leq 11$) in the Thue-Morse SL. Again they correlate well with the magnitude of transmission dips shown in Fig. 2(a).

The result for the single-layer Thue-Morse SL is shown in Fig. 3(a), where we have assumed $d_A = d_B = 20$ Å and the (001)-oriented ALAs and GaAs as the constituents of the A and B blocks, respectively. This choice of blocks is exactly the same as that for the SL sample fabricated and used in the experiment by Merlin *et al.*[9] Almost all dips in transmission found in Fig. 3(a) are labeled in the same way as in Fig. 2(a). The only modification needed is to replace ω by ω'. Here we note that the dips labeled by α and ϵ occur at $\omega = \omega'_z$, where $z = \frac{1}{3} + \frac{3}{8}$ and $z = \frac{5}{3} - \frac{3}{8}$, re-

TABLE I. Spectral intensities at frequencies $\nu_m = \omega_m / 2\pi$ in the double-layer AlAs/GaAs SL's. The phonon mode is TA.

m	ν_m (GHz)	$\lvert f_+\rvert^2/4$ ($\propto \lvert S^{\mathrm{TM}}\rvert^2$)	$\lvert f\rvert^2$ ($\propto \lvert S^P\rvert^2$)
1	184	0.018	0.13
2	368	0.77	1.47
3	551	2.72	3.29
4	735	2×10^{-5}	0.007
5	919	1.21	1.35
6	1102	0.02	0.05
7	1286	0.02	0.09
8	1470	2.12	2.14

TABLE II. Spectral intensities at frequencies $\nu_z=\omega_z/2\pi$ ($z=m/3$) in the double-layer Thue-Morse SL. The phonon mode is TA.

z	ν_z (GHz)	$\lvert f_-\rvert^2/4$ ($\propto \lvert S^{\mathrm{TM}}\rvert^2$)
$\frac{1}{3}$	61	0.007
$\frac{2}{3}$	122	0.10
$\frac{4}{3}$	245	1.09
$\frac{5}{3}$	306	1.97
$\frac{7}{3}$	429	3.21
$\frac{8}{3}$	490	3.01
$\frac{10}{3}$	612	1.25
$\frac{11}{3}$	674	0.43

spectively. Actually, in the binary representation $\frac{3}{8}=0.011$ and $z=m/3+(\frac{1}{2})^k$ is not sufficient to label all small dips characteristic of the Thue-Morse SL's. A remarkable aspect observed in the transmission spectra of phonons in the single-layer SL is that most of the dips at $\omega'_{m/3}$ are larger than the dips at ω'_m. It should be noted that in the double-layer SL the dips at ω_m dominate those at $\omega_{m/3}$.

For comparison's sake we have also shown in Fig. 3(b) the corresponding result for the periodic SL consisting of the sequence $ABABAB\cdots$ of the same building blocks. Because a unit period $d_A+d_B=40$ Å much shorter than 96 Å ($=d_1^A+d_2^A+d_1^B+d_2^B$) of the double-layer SL is assumed, only three Bragg dips are found in Fig. 3(b) in the frequency range 0 THz to 1.5 THz, whereas eight dips are found in Fig. 2(b). Now, we observe that the correlation in the magnitude of transmission dips due to Bragg reflection is not evident between these single-layer Thue-Morse and periodic SL's, although they still occur at the same frequencies. This is because the single-layer Thue-Morse SL has a complicated unit-cell structure as described in the previous subsection, i.e., the effective unit blocks are not A and B but rather $\tilde{A}$ and its complement $\tilde{B}$ involving 16 original A and B blocks.

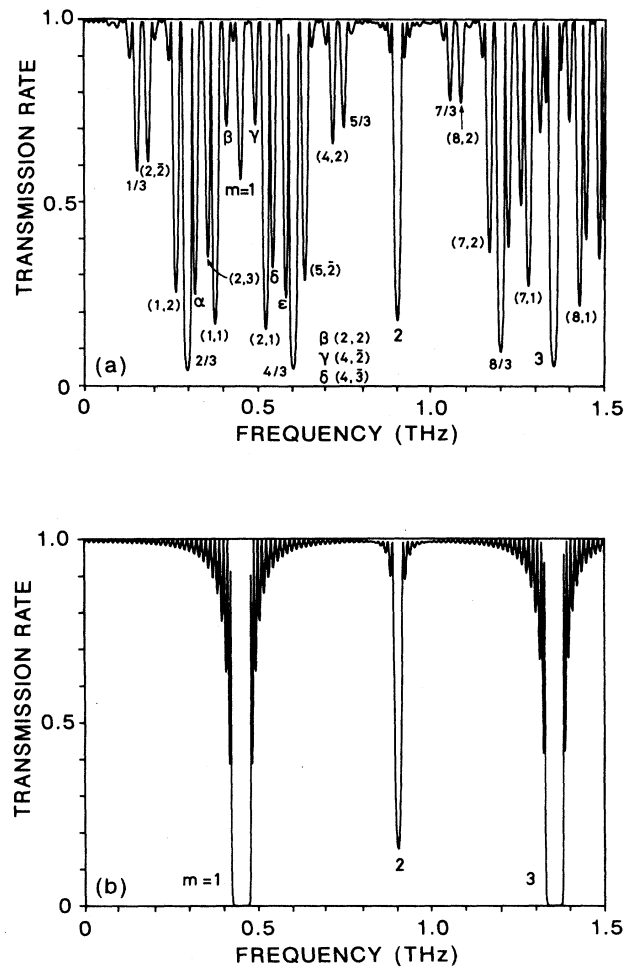

FIG. 3. Frequency dependence of TA-phonon transmission rate in single-layer (001)-oriented AlAs/GaAs SL's. Propagation is normal to the SL interfaces. (a) Thue-Morse SL. (b) Periodic SL. Thicknesses of blocks are $d_A=d_B=20$ Å, and the second generation with 64 original A and B blocks is assumed. Dips are labeled by the indices of the frequencies predicted by the structure factors (see the text).

TABLE III. Spectral intensities at frequencies $\nu_z=\omega_z/2\pi$ ($z=m$ and $m/3$) in the single-layer SL's. The phonon mode is TA.

z	ν_z (GHz)	$\lvert g_+/16\rvert^2$ ($\propto \lvert s^{\mathrm{TM}}\rvert^2$)	$\lvert g/8\rvert^2$ ($\propto \lvert s^P\rvert^2$)	$\lvert g_-/16\rvert^2$ ($\propto \lvert s^{\mathrm{TM}}\rvert^2$)
$\frac{1}{3}$	151			0.11
$\frac{2}{3}$	301			0.93
1	452	0.07	3.93	
$\frac{4}{3}$	603			0.875
$\frac{5}{3}$	753			0.07
2	904	0.27	0.29	
$\frac{7}{3}$	1055			0.04
$\frac{8}{3}$	1205			0.66
3	1356	0.53	3.37	

Table III shows the spectral intensities calculated from the structure factors at $\omega = \omega'_m$ and $\omega'_{m/3}$. The relative magnitudes of transmission dips in the single-layer SL's are again well described in terms of the spectral intensities given in this table. Thus, the structure factors we have derived successfully predict the properties of the transmission spectra (i.e., both the frequency and magnitude of transmission dips) of phonons in the Thue-Morse SL's.

V. FREQUENCY SPECTRA

As in the case of quasiperiodic systems,[3,24] an important insight into the spectral properties of phonons in a Thue-Morse SL would also be gained by studying the dispersion relations in this aperiodic layered system. They can be calculated by imposing a Bloch-like boundary condition on the acoustic fields in the SL. A similar boundary condition has been used to obtain the dispersion relations in a Fibonacci SL.[3] In the present calculation we have assumed an infinite repetition of a large "unit cell" which involves 124 blocks (corresponding to the seventh original generation) making up a Thue-Morse sequence.

Figures 4(a) and 4(b) show the dispersion relations of both LA and TA phonons propagating normal to the double- and single-layer Thue-Morse SL's assumed in Sec. VI, respectively. In order to get these plots we have calculated the wave number for 5000 frequencies evenly distributed between 0 and 1 THz. If the wave number calculated is real, the chosen frequency is in an allowed band and a traveling wave is associated. However, if it is complex the corresponding frequency is in a forbidden gap and no traveling wave is excited. Note that in each figure the dispersion curve of the LA branch acts as the magnification of the low-frequency part of the TA branch.

A number of distinct frequency gaps can be seen as expected in the discussion developed in Sec. III. All these frequency gaps are confirmed to occur at frequencies Ω_m, $\Omega_{m/3}$, and $\Omega_{m/3+\Delta}$, where $\Omega = \omega$ or ω', and they have one-to-one correspondences to the dips in transmission shown in Figs. 2(a) and 3(a). Moreover, the gap width correlates well with the magnitude of the corresponding transmission dip. Accordingly we can also label the frequency gaps in the dispersion curves by the same indices as we have used to label the transmission dips. Thus, the dispersion relations provide complementary information on the spectral properties of phonons in the Thue-Morse SL's based on a nonperiodic, deterministic sequence.

One of the interesting problems on the spectral properties in the Thue-Morse SL is the fate of the frequency gaps at $\Omega_{m/3}$ (and also at $\Omega_{m/3+\Delta}$) in the $N \to \infty$ limit. As the generation number increases the spectral intensities or peaks at these frequencies grow in proportion 3^N, while they grow as 4^N at Ω_m. Hence the former peaks vanish relative to the Bragg peaks. However, the situation is not so simple. Based on a perturbative argument, Cheng *et al.*[13] suggested that those gaps will persist even in an infinite system probably related to the appearance of additional small spectral peaks arbitrary close to $\Omega_{m/3}$.

In order to gain an insight into this basic issue we have investigated numerically the TA-phonon dispersion relation in more detail. Here, the double-layer AlAs/GaAs

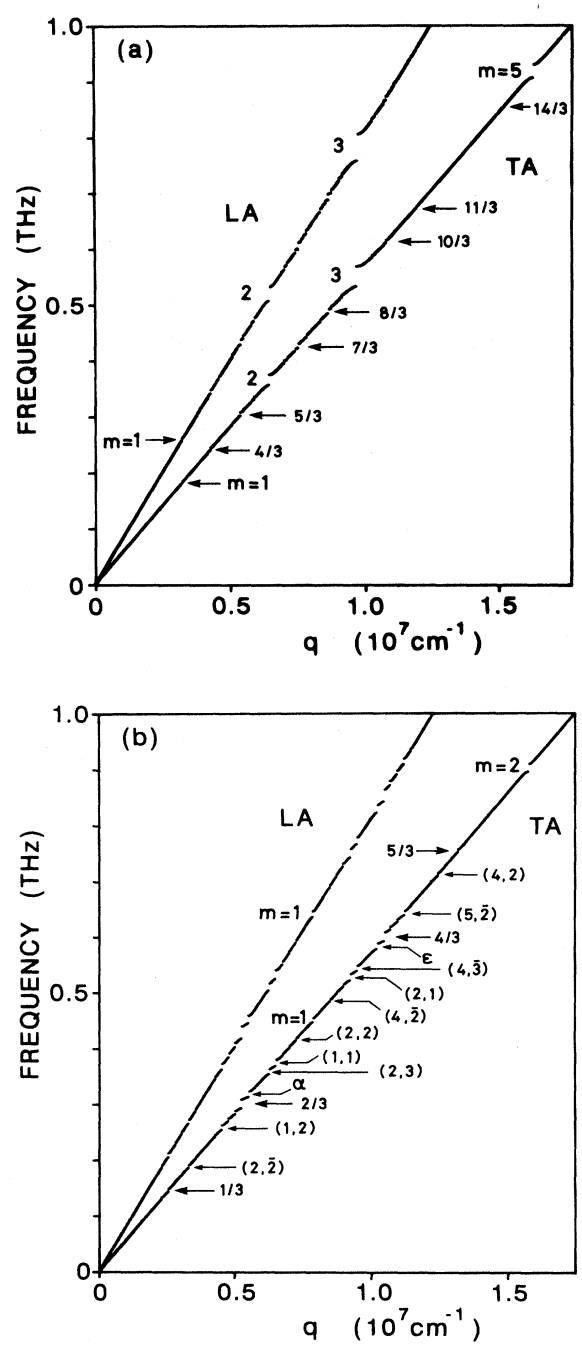

FIG. 4. Dispersion relation of phonons propagating normal to the interface of the same (001)-oriented AlAs/GaAs SL's as in Figs. 2 and 3. (a) Double-layer Thue-Morse SL. (b) Single-layer Thue-Morse SL. The frequency gaps are labeled in the same way as in Figs. 2 and 3.

SL [cf. Fig. 4(a)] is assumed. The magnifications of a portion of the dispersion curve involving both $\omega_{7/3}$ and $\omega_\tau = \omega_{8/3-1/4}$ are displayed in Fig. 5 for three different generations. Note that the ninth and eleventh generations of the Thue-Morse SL consist of 512 blocks (1024 layers) and 2048 blocks (4096 layers), respectively. Now, comparing the plots for the ninth and tenth generations the subdivision of allowed frequency bands is clearly seen in the dispersion curve of the higher generation. More specifically, each larger band is split into three smaller bands as the generation number increases. At the same time the diminishing or disappearance of certain bands is also recognized. These changes should be arising from the occurrence of additional small frequency gaps and associated reorganization of the former bands.

The same hierarchical behavior of the band structure proceeds as the generation number further increases (cf. the dispersion curve in the eleventh generation). Remarkably, however, the width of the large frequency gap in which $\omega_{7/3}$ is found does not exhibit any tendency to diminish with increasing the generation number. A similar result is also seen for the smaller gap in which ω_τ is involved. For comparison's sake, the dispersion curve at frequencies close to ω_2 is plotted in the inset for the tenth generation. The structure of the band edges on either side of this large Bragg gap is quite stable and almost unchanged even when the generation number is varied. We have also confirmed numerically that the same consequence for the persistence of the band gaps is valid at $\omega = \omega'_{m/3}$ in the single-layer SL. Combining the above results with the fact that $(\frac{3}{4})^N = 0.042$ for $N = 11$, it is quite probable that the frequency gaps at $\omega_{m/3}$ (also $\omega'_{m/3}$) with $m \neq 3n$ still persist in the $N \to \infty$ limit of the Thue-Morse SL.

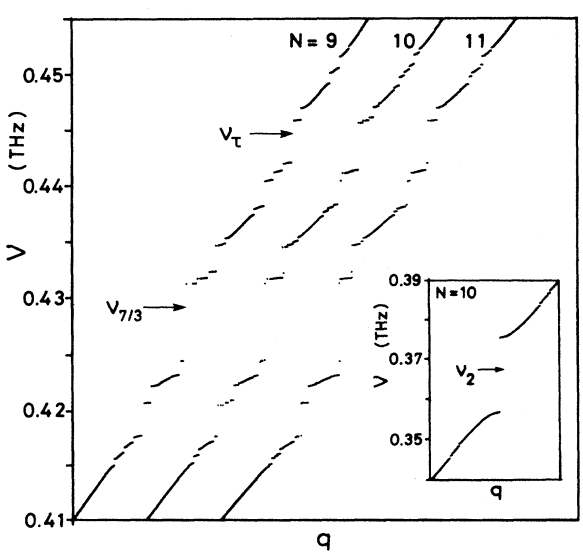

FIG. 5. Generation-number (N) dependence of the TA-phonon dispersion relation in a frequency region covering the frequency gaps in the vicinity of $\nu_{7/3}$ and $\nu_\tau = \nu_{8/3-1/4}$ ($\nu = \omega/2\pi$). The double-layer SL and normal incidence [the same as Fig. 4(a)] are assumed. These plots are obtained by calculating the wave numbers q for 10^4 to 2.5×10^4 frequencies equally spaced from 0.410 to 0.455 THz. Inset shows the dispersion curves in the vicinity of ν_2 for the tenth generation.

VI. ANGULAR DEPENDENCE OF THE TRANSMISSION RATE

So far, we have shown the results for phonons propagating parallel to the growth direction of SL's. For oblique phonon propagation, the situation becomes much more complicated. Mode conversions occur among three different polarizations of phonons by the reflection and transmission at SL interfaces. An important result of the mode conversion at the oblique propagation is the occurrence of intermode phonon-Bragg reflection in addition to ordinary intramode Bragg reflection. This has been established for phonons in the periodic[5] and quasiperiodic[3,4] SL's both theoretically and experimentally.

We expect the similar intermode reflections to occur in the Thue-Morse SL's. Figure 6(a) exhibits the angular dependence of the LA-phonon transmission rate in the double-layer Thue-Morse SL assumed in Sec. IV. The frequency is fixed to 850 GHz, i.e., the threshold frequency of PbBi tunnel junction used as a phonon detector,[5] and the propagation plane is 22.5° rotated away from both the (100) and (110) crystal plane of GaAs layer. (Note that GaAs is usually used also for a substrate of AlAs/GaAs SL). Several distinct dips in transmission can be seen in the angular dependence as well. Comparing Fig. 6(a) with Fig. 6(b) which shows the same transmission rate in the corresponding periodic double-layer SL, we recognize a remarkable correlation in major transmission dips in these systems. More specifically, all transmission dips in the periodic SL have their counterparts in the Thue-Morse SL, i.e., the dips appearing at the same propagation angles with very similar magnitude and width. A close correlation in the spectral properties of phonons found previously[3,4] in the periodic and quasiperiodic SL's with double-layer structure has recently been established theoretically.[21] Because all transmission dips in the periodic SL are due to Bragg reflection, those correlated dips in the Thue-Morse SL are also due to Bragg reflection originating from the periodicity discussed in Sec. III. In Fig. 6(b) we have indicated the reflection processes and the order of the reflection. Similarly, the origins of the transmission dips truly characteristic of the nonperiodicity of the Thue-Morse sequence are equally identified and labeled in Fig. 6(a).

These identifications of the transmission dips can be made by slightly extending the discussion given in Sec. III. Here we may only note that the wave number k_n defined there is the normal component of the wave vector in the nth layer. Hence, in the double-layer SL the transmission dips or frequency gaps at oblique propagation of phonons of frequency ω are predicted to appear at angles satisfying

$$2\omega\left[\frac{d_1^A + d_1^B}{v_1}\cos\theta_1 + \frac{d_2^A + d_2^B}{v_2}\cos\theta_2\right] = 2\pi z \ , \qquad (23)$$

where $z=m$, $m/3$, and $m/3+\Delta$, and θ_1 and θ_2 denote the polar angles of the wave vectors in the first and second layers (in the wave-vector space). In Eq. (23) v_1 and v_2 are the sound velocities in these directions. It should be remarked that both θ_1 and θ_2 are different from θ representing the polar angle of the group-velocity vector owing to the presence of the elastic anisotropy of the constituent layers. The quantities θ and v in the layers are further related to each other by Snell's law

$$\frac{v_1}{\sin\theta_1}=\frac{v_2}{\sin\theta_2}\ , \tag{24}$$

which is the manifestation of the translational symmetry of the system in the direction parallel to the interfaces.

Several transmission dips due to intermode-phonon-reflection processes are indicated in both Figs. 6(a) and 6(b). For the intermode reflections between the longitudinal and transverse modes Eq. (23) should be modified as

$$\omega\sum_{n=1}^{2}(d_n^A+d_n^B)\left[\frac{\cos\theta_n^{\rm L}}{v_n^{\rm L}}+\frac{\cos\theta_n^{\rm T}}{v_n^{\rm T}}\right]=2\pi z\ , \tag{25}$$

which is supplemented by

$$\frac{v_n^{\rm L}}{\sin\theta_n^{\rm L}}=\frac{v_n^{\rm T}}{\sin\theta_n^{\rm T}}\ , \tag{26}$$

together with Eq. (24). Here, L and T stand for the longitudinal and transverse modes, respectively. The intermode reflections between two different TA modes are also possible in SL's.

The angular dependence of the LA-phonon transmission rate in the single-layer Thue-Morse SL is shown in Fig. 7(a). Significant dips in transmission are equally observed. Comparing Fig. 7(a) with Fig. 7(b) exhibiting the

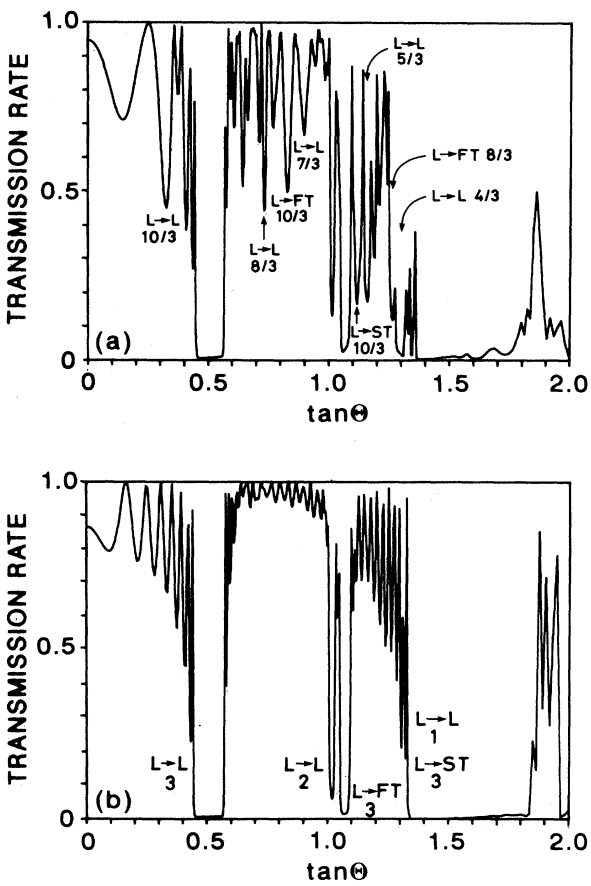

FIG. 6. Angular dependence of LA-phonon transmission rate in the double-layer (001)-oriented AlAs/GaAs SL's assumed in Fig. 2. (a) Thue-Morse SL. (b) Periodic SL. Frequency is 850 GHz. θ indicates the polar angle (in the real space) measured from the normal to the SL, i.e., the [001] axis, and in the plane 22.5° rotated away from both (100) and (110) planes. (a) The prominent dips other than those due to Bragg reflection are labeled by the reflection processes together with the indices related to the reflection.

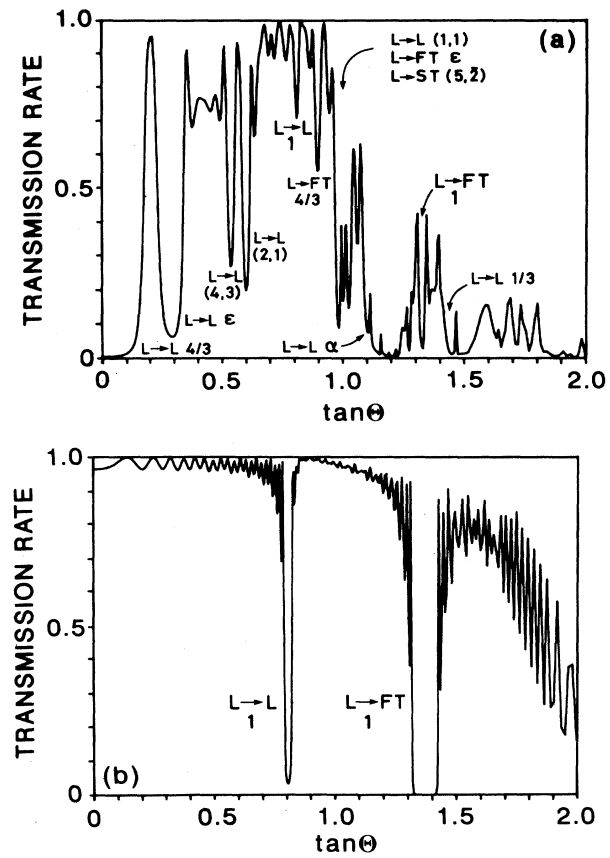

FIG. 7. Angular dependence of LA-phonon transmission rate in the single-layer (001)-oriented AlAs/GaAs SL's assumed in Fig. 3. (a) Thue-Morse SL. (b) Periodic SL. Frequency is 850 GHz. θ indicates the polar angle (in the real space) measured from the normal of the SL, i.e., the [001] axis, in the plane 22.5° rotated away from both (100) and (110) planes. The reflection processes and the indices related to the reflection responsible for prominent dips are also indicated.

result for the periodic SL, the correlation in the magnitude of Bragg-reflection dips is not evident in these SL systems though the dips are still found at the same angles satisfying the Bragg condition. The reason for this is again attributed to the fact that the blocks $\tilde{A}$ and $\tilde{B}$ regarded as well-defined units for the Thue-Morse sequence in this SL are quite different from the original A and B blocks comprising the unit cell AB of the periodic SL.

All those dips in Figs. 7(a) and 7(b) are identified as in the case of double-layer SL by the equations similar to Eqs. (23)–(26), where v_1 and v_2 are replaced by v_A and v_B (the similar replacements are applied for θ), and $d_1^A + d_1^B$ and $d_2^A + d_2^B$ by d_A and d_B, respectively. In this SL system the main transmission dips found in the angular dependence are those associated with the characteristic frequencies $\omega'_{m/3}$ and $\omega'_{m/3+\Delta}$ rather than ω'_m. The same result has been seen in the frequency dependence of the transmission. Note that the transmission dips due to intermode reflections are also recognized in both Figs. 7(a) and 7(b).

Phonon imaging has proved to provide an ideal tool to exploit experimentally the angular dependence of quasimonochromatic phonon transmission in SL's.[4,5] The transmission dips characteristic of the aperiodic Thue-Morse sequence would rather easily be observed experimentally by using the single-layer SL as a sample. This is because major transmission dips in the double-layer Thue-Morse SL are related to the Bragg reflection due to periodicity. (The fine dips are difficult to resolve experimentally by the limited frequency and angular resolution of the current phonon detectors.) However, almost all major transmission dips in the single-layer Thue-Morse SL found here are truly characteristic of the nonperiodicity of the basic sequence, and so they would readily be detected by phonon imaging.

VII. CONCLUSIONS

The experimental realization of AlAs/GaAs Thue-Morse SL's by Merlin *et al.*[9] aroused our interest in the vibrational properties of the systems which are neither periodic, quasiperiodic, nor random. In this paper we have derived the SL structure factors and studied spectral properties of acoustic phonons in the Thue-Morse SL's. The phonon transmission dips and frequency gaps in these systems are found at frequencies Ω_m ($=\omega_m$ or ω'_m) associated with mth-order Bragg reflection and at $\Omega_{m/3} = \Omega_m/3$ as predicted by the structure factors. Much finer spectral structures also appear at $\Omega_{m/3+\Delta}$, where $|\Delta|$ is less than unity and has a finite-length binary representation. As the size of the system (or equally the generation number) increases, the distribution of fine spectral dips or gaps becomes increasingly dense.

An interesting problem is whether transmission dips and frequency gaps at $\Omega_{m/3}$ persist in the $N \to \infty$ limit. As the generation number increases the spectral intensities or peaks at Ω_m and $\Omega_{m/3}$ grow in proportion to 4^N and 3^N, respectively, and thus it is naively expected that the latter vanish relative to the former. However, Cheng *et al.* suggested that they will persist even in an infinite system.[13] Our numerical calculation seems to support their expectation.

Through this work we have considered both double- and single-layer SL's as prototypes. It is found that the main structures of the transmission and frequency spectra in the double-layer Thue-Morse SL rather resemble those in the corresponding periodic SL, and the spectral peaks at ω_m originated from the Bragg reflection dominate. In the single-layer SL, however, the spectral intensities at $\omega'_{m/3}$ unique to the aperiodicity of the sequence have larger magnitudes than those at ω'_m. This result suggests that the single-layer SL is more appropriate than the double-layer one for the experimental verification of the spectral structures characteristic of the Thue-Morse sequence.

Some areas for future studies on the Thue-Morse sequence might include further mathematical analysis of the spectra[25] and experimentally relevant studies on networks.[26]

ACKNOWLEDGMENTS

One of us (F.N.) is grateful to J. Peyriere and, especially, J. P. Allouche for many enjoyable conversations on the Thue-Morse sequence. This research at the University of California, Santa Barbara was supported in part by the U.S. Department of Energy under Contract No. DE-84-ER45108 and the U.S. National Science Foundation (NSF) through Grant No. PHY-82-17852, supplemented by funds from the U.S. National Aeronautics and Space Administration (NASA). The other one (S.T.) was supported by a Grant-in-Aid for Scientific Research from the Ministry of Education, Science, and Culture of Japan, No. 63550001.

*Address after December 1989: Physics Department, The University of Michigan, Ann Arbor, MI 48109-1120.

[1]R. Merlin, K. Bajema, R. Clarke, F.-Y. Juang, and P. K. Bhattacharya, Phys. Rev. Lett. **55**, 1768 (1985).

[2]For a recent review, see R. Merlin, IEEE J. Quantum Electron. **QE-24**, 1791 (1988).

[3]S. Tamura and J. P. Wolfe, Phys. Rev. B **36**, 3491 (1987).

[4]D. C. Hurley, S. Tamura, J. P. Wolfe, K. Ploog, and J. Nagle, Phys. Rev. B **37**, 8829 (1988).

[5]D. C. Hurley, S. Tamura, J. P. Wolfe, and H. Morkoç, Phys. Rev. Lett. **58** 2446 (1987); S. Tamura, D. C. Hurley, and J. P. Wolfe, Phys. Rev. B **38**, 1427 (1988).

[6]A. Thue, Norske Vidensk. Selsk, Skr. I. Mat.-Nat. Kl **7**, No. 1 (1906); **11**, No. 1 (1912).

[7]M. Morse, Trans. Am. Math. Soc. **22**, 84 (1921); Am. J. Math. **43**, 35 (1921).

[8]J. P. Allouche (private communication).

[9]R. Merlin, K. Bajema, J. Nagle, and K. Ploog, J. Phys. (Paris) Colloq. **48**, C5-503 (1987).

[10]M. M. Doria, F. Nori, and I. Satija, Phys. Rev. B **39**, 6802 (1989).

[11]F. Axel and J. Peryriere, C. R. Acad. Sci. **305**, 1 (1987); F. Axel, J. P. Allouche, M. Kléman, M. Mendes-France, and J. Peyriere, J. Phys. (Paris) Colloq. **47**, C3-181 (1986).

[12]J. P. Allouche and J. Peyriere, C. R. Acad. Sci. **302**, 1135 (1986).
[13]Z. Cheng, R. Savit, and R. Merlin, Phys. Rev. B **37**, 4375 (1988).
[14]M. Keane, Z. Wahrsch. Verw. Gebiete **10**, 335 (1968).
[15]A. Cobham, Math. Syst. Theor. **3**, 186 (1966); **6**, 164 (1972).
[16]G. T. Herman and G. Rozenberg, *Developmental Systems and Languages* (North-Holland, Amsterdam, 1975).
[17]G. Christol, T. Kamae, M. Mendes-France, and G. Rauzy, Bull. Soc. Math. France **108**, 401 (1980).
[18]F. M. Dekking, J. Comb. Theory Ser. A **27**, 292 (1976).
[19]M. W. C. Dharma-wardana, A. H. MacDonald, D. J. Lockwood, J. M. Barbibeau, and D. C. Houghton, Phys. Rev. Lett. **58**, 1761 (1987).
[20]S. Tamura and J. P. Wolfe, Phys. Rev. B **38**, 5610 (1988).
[21]S. Tamura and T. Watanabe, Phys. Rev. B **39**, 5349 (1989).
[22]V. Narayanamurti, H. L. Stormer, M. A. Chin, A. C. Gossard, and W. Wiegmann, Phys. Rev. Lett. **43**, 2012 (1979).
[23]O. Koblinger, J. Mebert, E. Dittrich, S. Dottinger, W. Eisenmenger, P. V. Santos, and L. Ley, Phys. Rev. B **34**, 2207 (1986).
[24]F. Nori and J. Rodriguez, Phys. Rev. B **34**, 2207 (1986).
[25]M. Kolář and M. K. Ali, Phys. Rev. B **39**, 426 (1989); Q. Niu and F. Nori, Phys. Rev. Lett. **57**, 2057 (1986).
[26]F. Nori *et al.*, Phys. Rev. B **36**, 8338 (1987); **37**, 2364 (1988); Physica B **152**, 105 (1988); Q. Niu and F. Nori, Phys. Rev. B **39**, 2134 (1989).